Active Plasma Uniformity Control Method: A Novel Meta Material with Photo-reactive Capacitance

Sungyoung Yoon[1], Meehyun Lim[1], Taekjin Kim[1], Sunghwi Cho[1], Jinyeong Yun[1], Sungyong Lim[1], Minyeul Lee[2], Jonghwa Shin[2] and Sungyeol Kim[1]

[1] *Mechatronics R&D Center, Samsung Electronics Co. Ltd, Samsungjeonja-ro, Hwaseong-si, Gyeonggi-do, Korea*
[2] *Department of Materials Science and Engineering, KAIST, Daejeon-si, Korea*

Abstract: An The importance of process uniformity is exponentially increasing because the process margins are getting tight and the ramp-up time of the yield depends highly on the process capability. Accordingly, many researches are being conducted, and many hardware knobs such as altered upper electrode, movable edge ring, multi-zone gas injection, and multi-zone heater, multi-zone antenna, and powered edge-ring are installed and used in process chambers. The researchers pursuing active control ability for Tool-to-Tool Match and mechanical motion-less for non-particle generation. In this context, this paper introduces a new meta-material with photo-reactive capacity. It is believed that this material, when applied as a boundary material in process chamber, can be used as a novel uniformity control knob through the spatially-distributed impedance control of plasma boundary. This material was developed and actually manufactured in collaboration with KAIST. Feasibility was verified by simulation and experiment. The results showed that the new material is able to control the 10% of plasma uniformity.

Keywords: Photo-reactive Meta-Material, Plasma Uniformity,

1. Introduction

Recently, semiconductor industry faces harsh challenge to make a step toward the next generation devices which need to be smaller, faster and more power-efficient than ever before. To satisfying tighter requirements in structures, such as CD (Critical Dimension) and HAR (High Aspect Ratio), the processes should reach to the extremely high accuracy and uniformity. To control the uniformity numerous technologies have been applied such as AUE (Altered Upper Electrode), segmented electrodes and TES (Tunable Edge Sheath) [1-3]. However, particle issue due to moving parts and passive control by electrical geometry are remained in unsolved issues.

Under this circumstances, one of key approaches to achieve better performance and productivity is to adopt a new meta-material which is having advantages in distributed control, no moving parts, active controllability and TTTM (Tool to Tool Match). To secure the uniformity in plasma-based semiconductor process equipment or precision in electro-magnetic field-based measuring equipment, it is necessary to control the electromagnetic field distribution in real time. In wafer etching equipment, especially, the non-uniformity of the electromagnetic field distribution caused by the presence of discontinuity of the material properties at the edge of the wafer can lead to deterioration of the etching quality at the edge of the wafer. Thus, one should reduce the non-uniformity to improve the process yield.

When a dielectric or conductive material is present adjacent to a position where an electromagnetic field to be controlled is present, a method of controlling an electromagnetic field is possible by changing variables such as shape, size, and position of the material or physical properties such as impedance.

This work studies how to control an electromagnetic field by light and developing a key material, "light-controlled variable dielectric material" by introducing the concept of meta-material, here after photo-reactive meta-material (PRM) [4]. This method is breaking away from traditional voltage application, electrode moving or fluid driving methods If this method is successful, in principle, independent electro-magnetic field control with high locality of 1 cm or less, electrical connection using metal or the like is not required, and mechanically moving parts are not required to ensure durability and reliability in extreme environments such as high temperature, high voltage, and high vacuum. It is also expected that the PRM is barely perturbed by RF power since the PRM is operated by light. In this case, the light from the plasma is should be blocked.

In the following chapters, we described the structure and mechanism of the PRM in-detail and then the results of the experiments were shown which is applied in international patent [5]. Based on the results, we drawn the conclusions in the final chapter

2. Mechanism and Design of PRM

The key components of PRM is are thin and wide metallic plates and semiconductor material that are stacked together with insulating dielectric spacer layers as shown in Fig. 1(a). The image of PRM substrate on sapphire glass is shown in Fig. 1(b). Here, the semiconductor material can be any material which shows the photoelectric effect. That is, emitting electrons and creating holes when applied the photon with certain energy. The energy of photon should be higher than the band gap of the semiconductor material. Since the semiconductor materials show different photon absorption coefficients with wavelengths, one should choose the suitable light source to operate the PRM.

There are many possible choices of plate shapes and lateral array configurations as shown in Fig. 2: (a) square pattern, top deposition, (b) strip pattern, top deposition, (c)

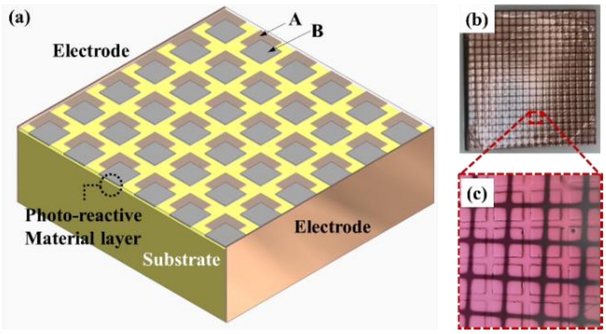

Fig. 1. (a) Structure of PRM. (b) Image of PRM. (c) Magnified view.

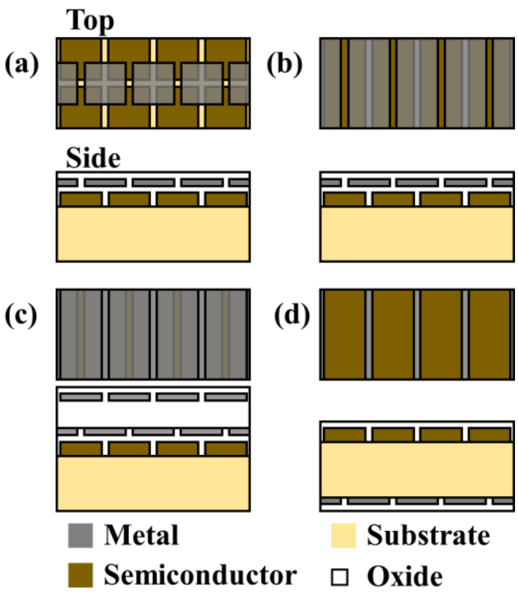

Fig. 2. Various structures of PRM: (a) Square pattern, top deposition, (b) strip pattern, top deposition, (c) strip pattern, top deposition, double metal layer and (d) strip pattern, top and bottom deposition.

strip pattern, top deposition, double metal layer and (d) strip pattern, top and bottom deposition.

Each has unique characteristics, pros and cons. In square pattern like Fig. 2(a), PRM will show identical ε_{eff} in two directions. The sprit pattern in Fig. 2(b-d) is easy to manufacture but shows different ε_{eff} with direction. On the number of metal layer number, the single metal layer in Fig. 2(a, b) is relatively free with chipping issue. That is, barely cracked in edge during dicing due to simple structure. The double metal layer structure in Fig. 2(c) has advantage in tanδ. The metal layer on the top will compensate the resistance in the semiconductor so that the tanδ will remained in low. However, the complex structure leads to chipping issues. Thus, in this work, we choose the strip pattern with top and bottom deposition. The simple and rigid structure is suitable for our research, lab-scaled feasibility test. Additionally, the semiconductor layer is covered with dielectrics to protect the layer from the exter-

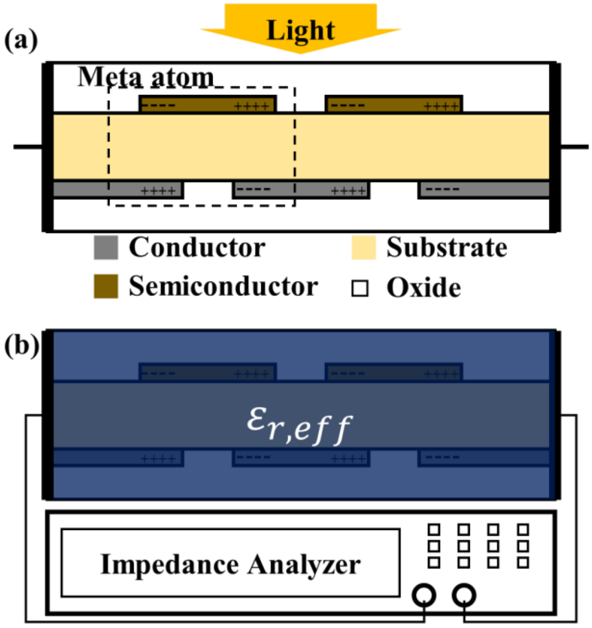

Fig. 3. (a) Diagram of PRM cross section and (b) Setup for effective relative permittivity measurement.

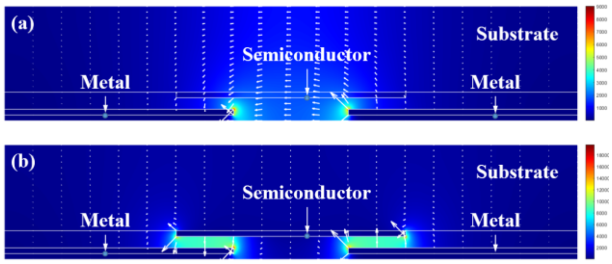

Fig. 4. Simulation of electric field intensity and vector in PRM metal atom: (a) without light and (b) with light.

nal damage or contamination. The protect layer should be transparent for suitable wavelength for photo-electric effect.

The detailed mechanism of permittivity change of PRM is described on Fig. 3(a) with sectional view PRM. The semiconductor and conductor form repeating patterns. The dashed square indicating a unit of the pattern. Since these patterns are gathered to form a meta-material, it is also called as "a meta-atom" [6]. When the light is applied on the material, electrons and holes from the photoelectric effect increase the charge carrier density in the semiconductor layer. The electric field change by the charge carrier in the semiconductor is simulated by using the MATLAB® as presented in the Fig. 4.

In Fig. 4, simulated electric field intensity and vector in PRM metal atom is noted with color and arrow, respectively. In case of Fig. 4(a) since the semiconductor acts as dielectric, the electric field diverse into substrate and the two thin metal layer becomes the counter electrode in capacitor. However, in the Fig. 4(b), the external light increases the charge carrier density and conductivity of semiconductor and the electric field is concentrated between the metal and semiconductor. The electric field in

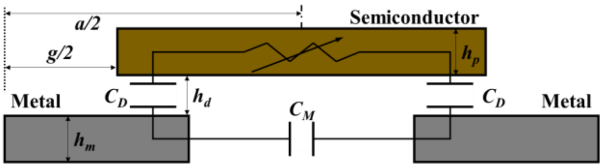

Fig. 5. Lumped circuit modelling on meta-atom of PRM. The resistor and capacitor are deduced from the dimension parameters, semiconductor thickness h_p, gap between semiconductor and metal h_d, metal thickness h_m, distance between semiconductors g, and center to center length of semiconductor, a.

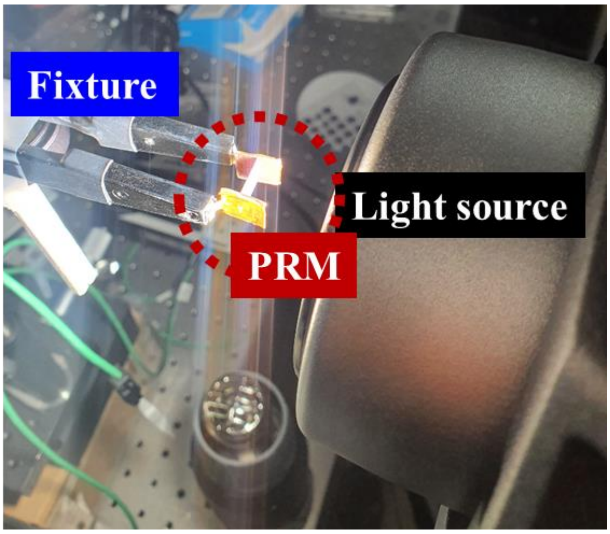

Fig. 6. Experiment setup for PRM feasibility test

the substrate becomes small enough to ignore. Consequently, the effective relative permittivity of substrate $\varepsilon_{r,eff}$, or ε_{eff} in short, is increased [7].

Based on the mechanism of PRM, one should able to design the dimension of PRM to meet the requirements in impedance control in semiconductor equipment as below:

1) Range of effective relative permittivity ε_{eff}
   Since the desirable range of ε_{eff} can be different with application target, the maximum or minimum value of ε_{eff} should be controllable.
2) Low tangential loss tanδ
   The tanδ means the resistance per inductance or capacitance of electrical component. Any non-perfect conductor has resistive component and leads to energy loss. In this work, we developed PRM for variable capacitor so that we want to minimize the tanδ.
3) Response time τ
   As mentioned in the Introduction chapter, the fast τ is necessary in various pulsed operations. In this work, we trying to secure the τ in tens of μs.

In order to deduce the design parameter, we developed the lumped circuit model as shown in the Fig. 5. The semiconductor is considered as perfect conductor in light on condition. Each capacitance between the metals and semiconductors CM and CD can be calculated from the

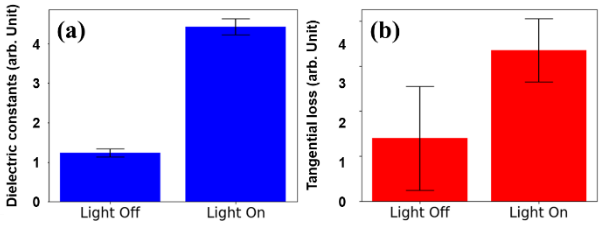

Fig. 7. Measured εeff (a) and tanδ (b) of PRM with/without light.

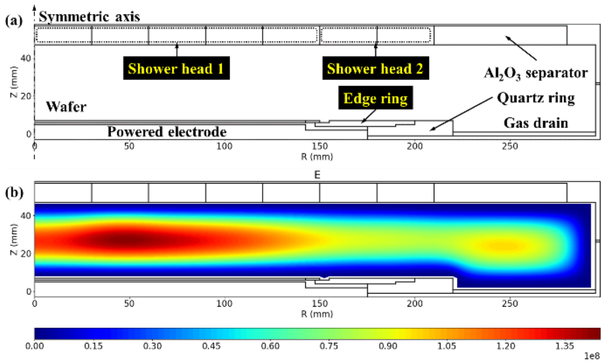

Fig. 8. (a) Diagram of HPEM simulation domain and example of electron density profile (εeff of shower head 1, shower head 2 and edge ring is equal to 10 in this case).

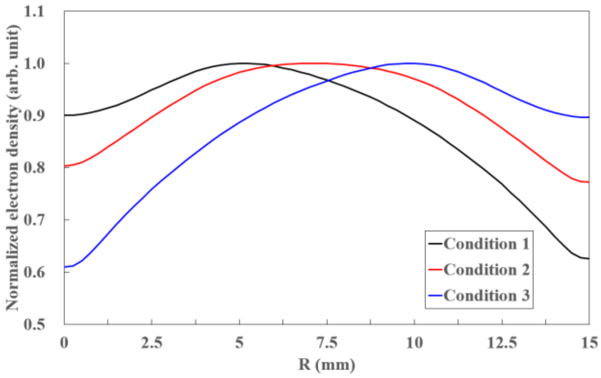

Fig. 9. Simulated electron density profiles.

known dielectric constant of oxide, SiO2 in this work, and geometry as in

$$C = \varepsilon_0 \varepsilon_d \frac{A}{d}, \tag{1}$$

where the ε_0, ε_r, A and d are vacuum permittivity, dielectric constant of oxide, overlapped area and distance, respectively.

From the capacitances, one can deduce the effective capacitance between two metals as

$$C_{eff} = \varepsilon_0 \frac{a(a-2g)}{4\mathrm{h}_d(\mathrm{h}_d+\mathrm{h}_m)} \varepsilon_d \frac{A}{a}. \tag{2}$$

By comparing (1) and (2), the εeff is in form of geometrical factor multiplied oxide dielectric constant like

$$\varepsilon_{eff} = \frac{a(a-2g)}{4\mathrm{h}_d(\mathrm{h}_d+\mathrm{h}_m)} \varepsilon_d. \tag{3}$$

Among the geometrical factor in (3), h_p plays important role in tangential loss tanδ and response time τ, because the two factors are in trade-off relation with h_p. As the thickness increasing, conductivity of semiconductor increases thus we can reduce the tanδ. However, the longer time is necessary in carrier generation and absorption with thickness thus the response time τ will getting slow [8].

Using numerical simulation, we decide the geometrical factors of PRM to secure the proper ε_{eff} and tanδ for semiconductor manufacturing plasma device.

3. Results and Discussion

The ε_{eff} and tanδ of PRM is measured as shown in Fig. 6. We used LED lamp and LCR meter for light source and electrical property measuring instrument. The measured results are shown in the Fig. 8. As shown in the Fig. 8, the ε_{eff} of PRM increased from by the photon 1.24±0.1 to 4.43±0.2 in arbitrary unit. Moreover, tanδ was remained under critical value in plasma device for semiconductor manufacturing. Thus the resistive power loss can be ignorable compare to the total applied power.

It implies that our design parameter based on circuit model successfully worked and is able to manufacture the PRM with demanded electrical performances.

Also, we checked the thermal effect on PRM. We changed the temperature of PRM without external light. The two parameters, tanδ and ε_{eff} was barely changed, and the temperature dependency of ε_{eff} was less than 0.01/K. Although the high temperature can generate the free electrons and holes in the semiconductor, it seems that the applied light played dominant role than the thermal effect. It implies that the PRM is suitable for general harsh thermal condition in semiconductor processing chamber.

Moreover, we tested the controllability of the PRM on the plasma uniformity by using the HPEM [9] which is plasma simulation software based on FORTAN. The schematic diagram of simulation domain is presented at Fig. 8(a). The shower head is divided into two regions with different electrical properties, relative permittivity ε_{eff}.

From the simulation, the plasma electron density $\underline{n}_e$ at the adjacent wafer surface for three difference simulation conditions are presented in Fig. 9. In Fig. 9, permittivity condition is distinguished as color of lines: black, red and blue lines are condition 1, 2 and 3, respectively. It seems that the ne was controlled ~30% by the PRM permittivity. When the PRM permittivity increases, the capacitance of component increase and impedance of component decreases. Thus the more power can be dissipated adjacent volume and the increase ne.

4. Conclusion

We developed the PRM and demonstrated the impedance control in substrate level. The PRM successfully increase the relative permittivity for RF frequency. We confirmed the effect of a shower head or edge ring made of PRM on plasma electron distribution by simulation. The results clearly show that the dielectric constant control by using PRM is able to control the plasma uniformity significantly. It is expected that the impedance controllable shower head or edge ring has advantages in development time because the short turn around period compare to structural control method such as electrode or shower head design change. The application field of PRM is not limited to the plasma chamber component. It can be developed as variable capacitor as an alternative method to vacuum variable capacitor or electrical variable capacitor.

Also, we expect that this method contributes to improving yield and cost reduction of next generation DRAM, FLASH and SoC devices.

Acknowledgements

This research was supported by Samsung Electronics.

5. References

[1] F. Andreas et al., U.S. Patent No. 9293926 (2016).
[2] B. Kallol, IEEE Trasn. On Plasma Sci., **38**, 11 (2010).
[3] R. Shahid et al., J Appl Phys., **107**, 093302 (2010).
[4] Chang, T. et al., Nature Comm., **7**, 12661 (2016)
[5] I. Kneppo et al., Solid State Electron, **15**, 5 (1972).
[6] J. Lee et al., U.S. Patent No. US17/335659 (2021).
[7] Nagai et al., Appl. Phys Appl. Phys. Lett. **110**, 172901 (2017).
[8] I. Katayama, Y. Ichikawa, and K. Tanaka, Phys. Rev. B **67**, 100102 (2003).
[9] M. J. Kushner, J. Phys. D. Appl. Phys., **42**, 19 (2009)